GEOLOGICAL JOURNAL
Geol. J. **37**: 97–115 (2002)
Published online in Wiley InterScience (www.interscience.wiley.com). DOI: 10.1002/gj.905

The Cretaceous volcanic succession around the Songliao Basin, NE China: relationship between volcanism and sedimentation

PUJUN WANG[1]*, YANGUANG REN[2], XUANLONG SHAN[1], SHAOBO SUN[1], CHUANBIAO WAN[2] and WEIHUA BIAN[1]

[1]*Earth Sciences' College, JiLin University, Changchun, PR China*
[2]*Daqing Exploration and Development Institute, Daqing, PR China*

With volume ratio of 8:1:1.5 amongst acidic, intermediate and basaltic rocks, the Cretaceous volcanics around the Songliao Basin are a series of high-K or medium-K, peraluminous or metaluminous, calc-alkaline rocks, lacking typical basalts and peralkaline members of typical rift-related types. Their eruption ages range between 133 and 127 Ma, 124 and 122 Ma and 117 and 113 Ma respectively. They are high in total (Rare earth element) REE contents (96.1–326 ppm), enriched in LREE and depleted in HREE (LREE/HREE = 4.6–13.8), with negative Eu and Ce anomalies (Eu/Eu* = 0.04–0.88; Ce/Ce* = 0.60–0.97). They have enriched large-ion lithophile elements (e.g. K, Ba, Th) and depleted high field strength elements (e.g. Nb, Ti and Y), suggesting a subduction-related tectonic setting. The volcanic activities migrated from south to north, forming a successively northward-stepping volcanic series and showing a feature significantly different from the overlying sedimentary sequence striking northeast. Thus, an overlap basin model was proposed. Accompanied by opening of the basin, the volcanogenic succession was formed at the block-faulting stage (131–113 Ma) owing to the closure of the Mongolia–Okhotsk ocean in the Jurassic and early Cretaceous, while the overlying sedimentary sequence was unconformably deposited at the spreading stage (Albian–Maastrichtian) owing to the oblique subduction of the Pacific plate under the Eurasian plate. The volcanic succession constitutes the lower unit of basin filling and is the forerunner of further basin spreading. Copyright © 2002 John Wiley & Sons, Ltd.

Received 11 September 2000; revised version received 9 July 2001; accepted 26 July 2001

KEY WORDS Cretaceous volcanics; Songliao Basin; northeast China; basin evolution; geochronology; geochemistry; tectonics

1. INTRODUCTION

Situated in northeast China (Figure 1), the Songliao Basin (SB) is the most important oil and gas-bearing basin of China owing to its annual oil production of over 50 million tons. The Cretaceous volcanic rocks exposed around the SB were mapped (1:200 000) during the 1960s and 1970s by the province Geological Surveys of Jilin and Heilongjiang, northeast China. Since then related studies were mainly focused on the local areas where coal deposits were developed intercalated in the Mesozoic volcanic/pyroclastic successions (in the southwest and southeast of the SB; Figure 1). Those unpublished 'inner printings' were summarized in the series of volumes of the Regional Geology (Jilin Geological Survey 1988; Heilongjiang Geological Survey 1993), and in the Geological Map of China (Cheng *et al.* 1990). In the 1990s, regional lithostratigraphic classification and correlation were done on the basis of the original mapping work (Jilin Geological Survey 1997; Heilongjiang Geological Survey 1997). In view of volcanic rocks in the area, the mapping and stratigraphic work emphasized the analysis of volcanic petrography and fossil assemblages contained in the epiclastic intercalations. These studies provided some general constraints

* Correspondence to: PuJun Wang, Earth Sciences' College, JiLin University, JianSheJie Str. 79 (Pigeon Building), 130061 Changchun, JiLin, PR China. E-mail: wpjslw@public.cc.jl.cn

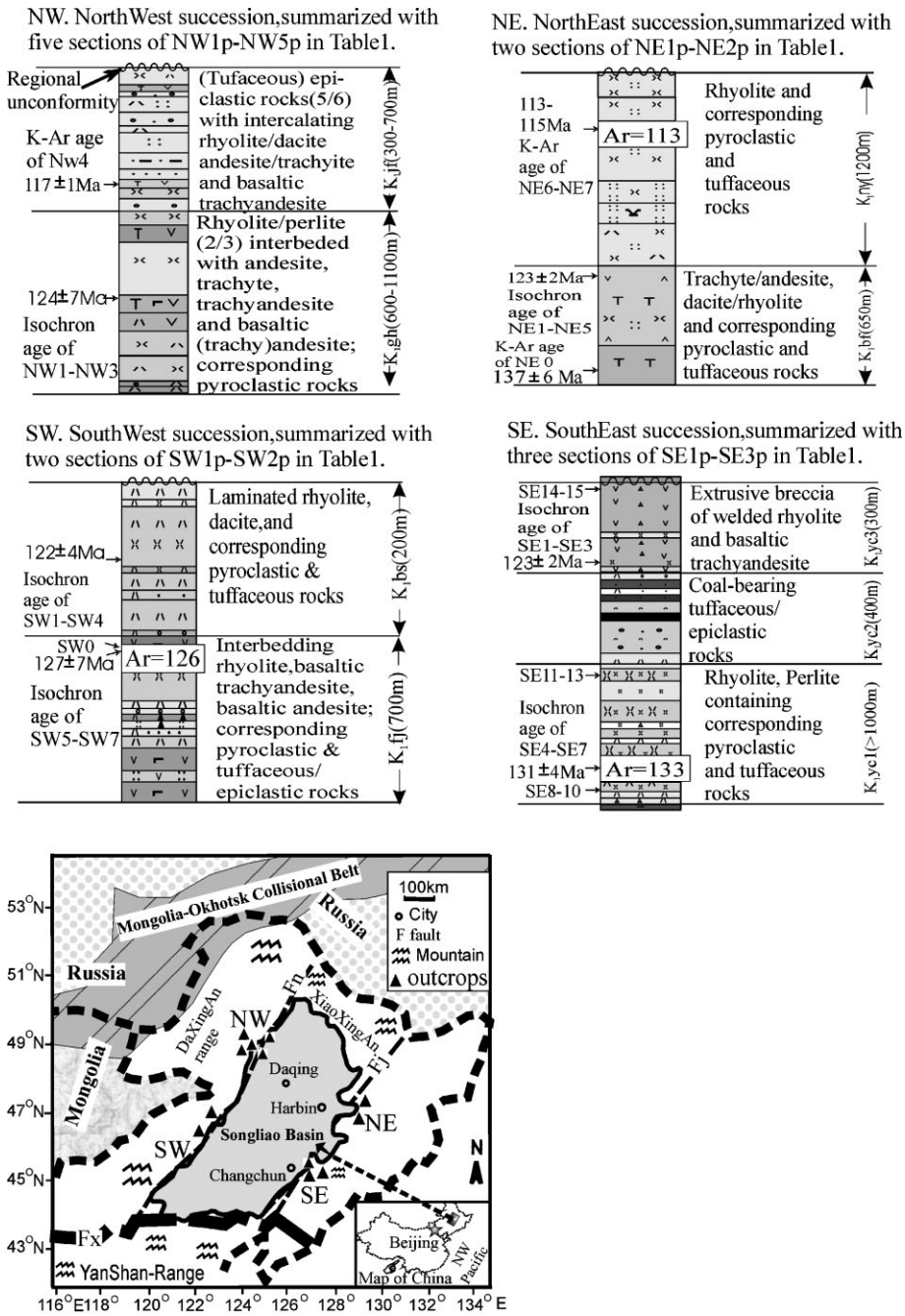

Figure 1. Schematic composite stratigraphic columns of the Cretaceous volcanogenic successions exposed around the Songliao Basin, northeast China. Relative positions of the outcrops in the basin are shown in the map. Their GPS spots and corresponding lithologic assemblages are listed in Table 1. Arrows on the left of the columns indicate positions of samples analysed for dating/geochemistry including three ^{40}Ar-^{39}Ar samples.

on the volcanic rocks (Song *et al.* 1999; Shan *et al*. 1999). Since precise dating was not available to classify all the volcanics, they had been mapped as Late Jurassic–Early Cretaceous (J_3–K_1) strata as a whole (Cheng *et al.* 1990). The tectonic meanings of the volcanics and their relation to the sedimentary basins in northeast China have recently attracted much attention (e.g. Li *et al*. 1997; Wang *et al*. 1997a; Zhu *et al*. 1997; Zhao *et al*. 1998).

However, there are hitherto very limited geochemical data on the volcanic rocks, and even less work has been done on their geochronology. The tectonic environment of emplacement of the volcanic rocks and their relation to the synchronously formed Songliao Basin are still questionable. The purpose of this paper is to investigate in detail the spatial and temporal variability in geochronology and geochemistry of the volcanic rocks, and evaluate the relationship between volcanism and genesis of the Songliao Basin, hoping to provide an example of the role of volcanism in sedimentary basin evolution.

2. GEOLOGICAL SETTING

The basement of the Songliao Basin (SB) was formed in the Permian consequent on suturing of the Xilamulun belt (Fx in Figure 1; Wang and Fan 1997; Zhang *et al.* 1999). Approximately 200–600 km north of the SB is the Mongolia–Okhotsk collisional belt formed during 152–94 Ma because of closure of the Mongolia–Okhotsk Ocean (alternatively called the Amurian Seaway; Scotese 1988; Zhao *et al*. 1990; Zorin 1999), which event had the closest time and space relationship to the volcanics studied in this paper. Along the eastern margin of the present SB is situated the Jiayi Fault zone (Fj in Figure 1), which is the northward extension of the Tanlu Fault zone formed by subduction of the Pacific Plate under the Eurasian Plate in the Late Cretaceous and Tertiary (Xu and Ma 1990; Ross *et al*. 1996).

The formation of the Xilamulun suture zone resulted in the assemblage of the pre-existing microterranes and constructed the pre-Mesozoic basement for the SB and adjacent areas (Zhang *et al*. 1999). The Mongolia–Okhotsk collisional belt caused the regional magmatic activities involving the study area (Khudoley and Sokolov 1998). The activation of the Jiayi Fault during late Cretaceous and Tertiary times had so great an influence on the area of the SB and its vicinity that it resulted in the uplift and erosion of the eastern part of the basin, intensively obscured all the pre-existing structures, and produced regional angular unconformities and inverse structures (Wang *et al*. 1993; Gao and Xiao 1995; Song 1997).

3. SAMPLING AND ANALYTICAL METHODS

Twelve sections of Cretaceous volcanic/pyroclastic successions were investigated with a measured accumulative thickness of 8800 m (Table 1). Over 450 samples were collected. Thin-section work was done on these samples. Thirty-five samples were carefully selected from the suite for K-Ar dating and/or geochemical research in this paper (Tables 2 and 3). Isotopic dating (especially for isochron ages) and geochemical studies were concentrated on several major volcanic bodies around the SB. The selected samples can represent general features of the volcanics of the region according to the regional distribution and correlation (Heilongjiang Geological Survey 1997; Jilin Geological Survey 1997).

Bulk chemical compositions and trace elements were determined with conventional chemical methods and X-ray fluorescence techniques respectively, at the analytical centre of Changchun University of Science and Technology. Rare earth element (REE) analyses were performed with ICP-AES after being pre-concentrated at Jilin Institute of Geology. The Regional Geochemical Exploration Standard (China National Standard Samples and Directions, 1984, unpublished) was analysed during the determination of the samples. Analytical procedures and detection limits for the elements are similar to those described by Wang *et al.* (1997b). K-Ar isotope dilution analyses and ^{40}Ar-^{39}Ar step-heating were performed at Geological Institute of Chinese Academy, Beijing, using the procedures described by Wang *et al.* (1983) and Sang *et al*. (1997).

Table 1. The Cretaceous volcanogenic successions exposed around the present Songliao Basin

ID[1]	GPS-spot	Thickness (m)	Formation[2]	Rock assemblage[3] (thickness %)	Transitional form[4] (frequency %)	Lithofacies[5]
NW1p	N47°18.068 E122°53.973	620	K1gh	BTan (62) Ande & Trac/Tand (3) Rhyo (35)	BTan → Rhyo (53) BTan → Ande/ Trac (33) BTan → Ande → Rhyo (7) Ande/Trac → Rhyo (7)	Lava + Ignim; *bimodal-like*
NW2p	N47°13.497 E122°59.136	1160	K1gh	BTan (5) Rhyo & Perl (95)	Rhyo → BTan → Rhyo (100) i.e. BTan in Rhyo	Lava + Ignim *bimodal-like*
NW3p	N47°12.313 E122°56.739	590	K1gh	BTan (45) Ande & Trac (19) Rhyo (23) Clas (13)	Rhyo → BTan (50) Ande/Trac in Clas (33) Rhyo in Clas (17)	Lava + Ignim + Fluv
NW4p	N47°18.539 E122°40.094	250	K1jf	BTan (4) Ande (11) Rhyo (15) Clas & Coal (70)	BTan → Rhyo (30) Ande → Rhyo (20) Rhyo → BTan (10) Ande in Clas (40)	Lava + Ignim + Fluv
NW5p	N47°18.316 E122°42.357	630	K1jf	Rhyo & Daci (56) Ande & Trac (7) Clas & Coal (37)	Frequent interbedding of volcanic-clastic rocks	Lava + Ignim + Fluv
SW1p	N45°47.065 E121°47.772	210	K1bs	Rhyo/Daci (25) Pcla (50) Clas (25)	Rhyo/Daci in graded bedding pyroclastic and laminated clastic rocks	Ignim + Fluv
SW2p	N45°48.373 E121°45.110	690	K1fj	Rhyo (40) BTan/Band (15) Pcla & Clas (45)	BTan/Band → Rhyo (30) Interbedding of volcanite -Pcla-Clas (70)	Ignim + Fluv Locally *bimodal-like*
SE1p	N44°23.061 E126°09.657	>2000	K1yc	Rhyo/Daci (65) BTan (10) Pcla + Clas & Coal (25)	BTan-Rhyo (upper) Pcla-Clas (middle) Rhyo-Pcla (lower)	Bimodal-like (upper) Allu + Fluv (middle) Lava + Ignim (lower)
SE2p	N44°28.958 E126°21.611	>600	K1yc	Rhyo/Perl (70) Pcla/Tuffite (30)	Pcla/tuffite (upper) Rhyo (middle) Perl (lower)	Lava + Ignim
SE3p	N44°09.800E 125°54.000	>200	K1yc	Rhyo/Perl (40) Pcla/Tuffite (60)	Pcla/tuffite (upper) Rhyo (middle) Perl (lower)	Lava + Ignim
NE1p	N45°35.217 E127°36.661	650	K1bf	Daci/Rhyo (40) Trac/Ande (60)	Transitional of massive intermediate-acidic rocks	Lava + Ignim
NE2p	N45°42.033 E127°45.871	1200	K1ny	Rhyo/Daci (100)	Rhythmic of massive-laminated acidic rocks	Lava + Ignim

[1]NW, SW, NE, SE = outcrops exposed northwest, southwest, northeast and southeast of the Songliao Basin.
[2]All the rocks are Cretaceous, but they have been given different local names as indicated.
[3]Key: Rhyo, rhyolite; Perl, perlite; Daci, dacite; ande, andesite; Trac, trachyte; Tand, trachyandesite; Band, basaltic andesite; BTan, basaltic trachyandesite; Pcla, pyroclastic deposits; Clas, epiclastic sediments; Coal, coal beds.
[4]Upward sequential change of rocks.
[5]Lithofacies: Lava, lava flow facies; Ignim, ignimbrites; Fluv, fluvial deposits; Allu, alluvial fan.

Table 2. K-Ar data on the whole volcanic rocks around the Songliao Basin

No	Sample	Weight (g)	K (%)	$^{40}Ar^*$ (10 E-10 mol/g)	^{40}Ar (rad) (%)	$^{40}Ar/^{40}K$	Age (Ma)
NW1	Andesite	0.2103	0.63	1.469	85.6	0.007792	129.3 ± 1.5
NW2	Andesite	0.1867	1.31	2.913	86.7	0.007431	123.5 ± 1.3
NW3	Trachyandesite	0.1712	1.26	2.89	89.3	0.007665	127.3 ± 1.3
NW4	Trachyte	0.1579	4.18	8.778	93.6	0.007017	116.9 ± 0.8
SW1	Dacite	0.0824	2.98	7.032	87.4	0.007885	130.8 ± 1.6
SW2	Rhyolite	0.0831	2.28	5.069	89.6	0.007429	123.5 ± 1.3
SW3	Rhyolite	0.0805	3.09	7.029	91.0	0.007601	126.3 ± 1.4
SW4	Rhyolite	0.0797	3.1	6.995	91.4	0.007540	125.3 ± 1.3
SW5	Rhyolite	0.0715	3.57	8.884	87.9	0.008316	137.7 ± 1.7
SW6	Basaltic andesite	0.15	1.95	4.84	90.4	0.008298	137.4 ± 1.7
SW7	Rhyolite	0.1346	3.04	7.278	92.4	0.008000	132.7 ± 1.3
NE0	Trachyte	0.1585	2.97	7.351	91.0	0.008271	137.0 ± 6.2
NE1	Trachyte	0.0501	3.19	7.124	88.7	0.007463	124.0 ± 1.3
NE2	Dacite	0.0609	2.93	6.753	89.1	0.007702	127.9 ± 1.4
NE3	Trachyte	0.0644	2.87	6.467	90.2	0.007530	125.1 ± 1.2
NE4	Dacite	0.0719	2.86	6.556	90.9	0.007660	127.2 ± 1.3
NE5	Rhyolite	0.0812	3.02	6.635	94.2	0.007342	122.1 ± 1.0
NE6	Rhyolite	0.0639	4.27	8.693	93.3	0.006803	113.4 ± 1.2
NE7	Rhyolite	0.0781	3.81	7.893	94.1	0.006923	115.3 ± 1.1
SE1	Rhyolite	0.0689	1.92	4.22	88.4	0.007345	122.1 ± 1.3
SE2	Rhyolite	0.0358	4.51	10.08	90.4	0.007469	124.1 ± 1.2
SE3	Rhyolite	0.0286	6.85	15.05	91.8	0.007342	122.1 ± 1.2
SE4	Rhyolite	0.0312	3.44	8.449	79.5	0.008208	136.0 ± 2.4
SE5	Rhyolite	0.1423	3.93	9.5624	87.7	0.008131	134.7 ± 5.8
SE6	Rhyolite	0.0377	2.38	6.013	89.0	0.008443	139.7 ± 1.9
SE7	Rhyolite	0.1395	3.76	9.142	91.3	0.008125	134.6 ± 1.7

Analysed in Beijing Geological Institute of Chinese Academy with RGA-10 Gas Mass-spectrometry of British VSS Company. $\lambda = 5.543e\text{-}10/year$.

4. PETROGRAPHY, SUCCESSION AND DISTRIBUTION

The volcanic rocks around the SB include rhyolite, dacite, trachyte, andesite, trachyandesite, basaltic andesite and basaltic trachyandesite (Figure 2). The volcanics are either metaluminous or peraluminous (Figure 3), medium-K or high-K (Figure 4), calc-alkaline series dominant (except two tholeiitic samples, Figure 5). The typical texture of the volcanic rocks is a low phenocryst porphyritic texture with complex phenocryst assemblage commonly including quartz, feldspars (sanidine, anorthoclase and plagioclase), biotite, hornblende, magnetite, ilmenite and pyroxene. The phenocrysts are generally less than 15% in volume of the volcanic rocks. Rock names and textures used in the paper follow Le Maitre *et al*. (1989), MacKenzie *et al*. (1982) and Shelley (1995).

The entire successions of the Cretaceous volcanic rocks around the SB range in thickness between 200 m and 2000 m (Figure 1 and Table 1). They begin with thick-massive bodies of widely distributed rhyolite and end with bimodal-like alternations of basaltic trachyandesite and rhyolite (SE in Figure 1). They can also begin with bimodal-like rhythms of basaltic trachyandesite–rhyolite and end with layered acidic volcanic rocks (SW and NW in Figure 1). Another type of succession is transitional with massive intermediate-acidic rocks in the lower part and uniform rhyolite/dacite in the upper part (NE in Figure 1).

The Cretaceous volcanic rocks around the SB are rhyolitic dominant with volume ratio of 8:1:1.5 amongst acidic (rhyolite/perlite and dacite), intermediate (trachyte and andesite) and basaltic rocks (basaltic andesite and basaltic trachyandesite). But the ratios change greatly from place to place. The volume percentages of basaltic trachyandesite as well as andesitic rocks increase with northerly latitude. In contrast, volume percentages of the pyroclastic rocks, which include pyroclastic rock and tuffites of Le Maitre *et al*. (1989), show a decreasing trend

Table 3. Major (wt%) and trace (ppm) elements and ratios of the representative Cretaceous volcanic rocks around the Songliao Basin

Sample Rock type	NW2 Andesite	NW4 Trachyte	SW2 Rhyolite	SW3 Rhyolite	SW6 Basaltic andesite	SW7 Rhyolite	NE0 Trachyte	NE1 Trachyte	NE5 Rhyolite	NE6 Rhyolite	SE2 Rhyolite	SE5 Rhyolite	SE6 Perlite
SiO_2	59.06	64.75	73.11	71.11	55.96	71.58	66.42	63.85	73.53	71.01	75.36	81.74	72.9
Al_2O_3	17.96	15.12	14.26	13.42	14.65	13.84	15.94	15.73	13.34	13.87	12.77	9.23	12.06
Fe_2O_3	3.24	3.78	1.31	1.26	4.22	2.79	1.91	1.78	1.78	2.15	1.44	0.61	0.54
FeO	2.21	0.76	0.55	1.31	2.83	0.48	1.99	2.48	0.35	0.56	1.24	0.43	0.24
MgO	1.82	1.26	0.49	1.01	4.04	0.62	3.85	1.75	0.34	0.57	0.28	0.44	0.12
K_2O	1.68	4.5	2.6	2.87	2.09	2.92	3.21	3.11	5.46	3.74	4.8	4.21	2.87
Na_2O	4.28	3.95	4.38	3.92	3.16	4.94	4.5	4.44	2.37	4.34	3.63	2.21	4.23
CaO	6.75	2.63	0.58	2.03	8.01	0.52	0.67	4.28	0.44	1.67	0.39	0.22	0.69
P_2O_5	0.28	0.18	0.1	0.1	0.3	0.18	0.05	0.24	0.1	0.12	0.03	0.03	0
MnO	0.11	0.07	0.02	0.04	0.12	0.02	0.14	0.11	0.02	0.08	0.03	0.03	0.06
TiO_2	0.74	0.64	0.7	0.35	0.78	0.47	0.54	0.67	0.27	0.42	0.17	0.04	0.1
LOI	1.91	1.82	2.15	2.75	3.68	1.61	0.53	1.52	2.25	1.45	0.32	0.71	5.96
Total	100.04	99.46	100.25	100.17	99.84	99.97	99.75	99.96	100.25	99.98	99.79	100.43	100.43
La (DL = 0.5 ppm)	28.91	28.68	33.33	28.2	21.74	24.86	51.21	37.51	40.34	36.47	69.54	36.45	31.97
Ce (DL = 1.0 ppm)	50.62	48.97	47.46	46.76	35.15	47.3	83.57	72.46	73.41	65.17	121.5	75.24	51.98
Pr (DL = 0.1 ppm)	7.22	4.2	10.15	7.56	7.61	6.06	9.46	12.91	10.11	5.61	17.03	8.59	6.11
Nd (DL = 0.5 ppm)	27.21	21.09	23.68	23.98	22.02	22.41	39.27	32.3	29.5	23.38	60.67	33.71	20.22
Sm (DL = 0.1 ppm)	5.66	3.63	4.12	4.21	4.81	4.63	7.58	6.58	5.36	4.43	12.37	7.91	3.57
Eu (DL = 0.005 ppm)	1.45	0.93	0.59	0.7	1.1	0.8	1.75	1.34	0.78	0.82	0.28	0.1	0.17
Gd (DL = 0.1 ppm)	4.51	2.64	2.67	3.12	4.93	3.96	5.9	4.59	3.64	3.2	11.57	6.8	2.94
Tb (DL = 0.01 ppm)	1.06	0.36	1.16	0.89	1.38	0.81	0.94	1.31	0.95	0.44	2.19	1.22	0.52
Dy (DL = 0.01 ppm)	3.76	2.01	2.58	2.92	5.05	3.79	5.74	4.01	3.31	4.01	13	7.78	3.11
Ho (DL = 0.008 ppm)	0.86	0.37	0.75	0.7	1.26	0.79	1.08	1.06	0.82	0.62	2.67	1.48	0.58
Er (DL = 0.01 ppm)	2.36	1.1	1.88	1.92	3.24	2.3	3.5	2.54	2.16	2.53	6.95	4.64	1.96
Tm (DL = 0.008 ppm)	0.46	0.17	0.52	0.4	0.72	0.4	0.5	0.64	0.48	0.27	1.15	0.66	0.28
Yb (DL = 0.005 ppm)	1.83	0.91	1.42	1.82	2.9	2.12	3.26	2.56	2.52	2.98	6.54	4.32	1.89
Lu (DL = 0.005 ppm)	0.31	0.15	0.28	0.3	0.51	0.33	0.51	0.4	0.38	0.38	0.93	0.6	0.3
Y (DL = 0.005 ppm)	19.12	11.18	12.54	15.39	27.84	19.37	31.85	23.89	21.31	24.28	72.02	39.6	16.02
Ba	990	860	700	680	500	450	960	1130	760	550	135	125	95
Th	30	7.5	10.5	5.8	12.5	4.4	9.4	12.5	12.5	12.5	16.5	16	9.4
Nb	13.5	7.6	12.5	9.7	18	9.6	14.5	18	22.5	12	68	32	29.5
Sr	1020	700	225	360	540	250	330	410	115	225	82	49	106
Zr	195	125	145	145	240	145	210	300	200	210	950	560	160
Sc	11	8.7	6	7.6	20.5	9.6	9	10.5	5.3	6.7	4	1.2	4
V	90	92	35	60	163	55	72	95	38	42	22	16	16
Ni	10.5	16	5.6	5.6	31.5	16	6.4	13.5	10.5	13.5	14	5.9	6.8
Co	18.5	14.5	5.7	8.7	35	11.5	6.6	15	10.8	9.5	10	14.3	7
ΣREE, (La-Lu)	136.2	115.2	130.6	123.5	112.4	120.6	214.3	180.2	173.8	150.3	326.4	189.5	125.6
ΣLREE/ΣHREE	7.9	13.8	10.5	9.2	4.6	7.3	8.9	9.5	11.1	9.4	6.2	5.9	9.8
Eu/Eu*	0.85	0.88	0.51	0.57	0.68	0.56	0.77	0.71	0.51	0.64	0.07	0.04	0.16
Ce/Ce*	0.80	0.94	0.60	0.74	0.64	0.88	0.84	0.77	0.83	0.97	0.81	0.97	0.82
Tb/Tb*	1.49	0.89	2.58	1.72	1.62	1.22	0.94	1.77	1.59	0.72	1.05	0.99	1.01
Tm/Tm*	1.53	1.18	2.20	1.49	1.64	1.26	1.03	1.75	1.43	0.68	1.19	1.03	1.02
Eu/Sm	0.26	0.26	0.14	0.17	0.23	0.17	0.23	0.20	0.15	0.19	0.02	0.01	0.05
$(La/Lu)_{CN}$	9.68	19.85	12.36	9.76	4.43	7.82	10.42	9.74	11.02	9.96	7.76	6.31	11.06
$(La/Sm)_{CN}$	3.21	4.97	5.09	4.22	2.84	3.38	4.25	3.59	4.74	5.18	3.54	2.90	5.64
$(Gd/Yb)_{CN}$	2.00	2.35	1.52	1.39	1.38	1.51	1.47	1.45	1.17	0.87	1.43	1.28	1.26
Fe_2O_3/FeO (in mole)	1.32	4.48	2.14	0.87	1.34	5.23	0.86	0.65	4.58	3.45	1.04	1.28	2.02
Mg* value	0.59	0.75	0.61	0.58	0.72	0.70	0.78	0.56	0.63	0.64	0.29	0.65	0.47

DL, detection limit; LREE = La-Sm; HREE = Gd-Lu; Eu* = $(Sm + Gd)_{Chondrite}/2$, similarly for Ce*, Tb* and Tm*; CN, chondrite normalized value; Mg* value = MgO/(MgO + FeO) in mole.

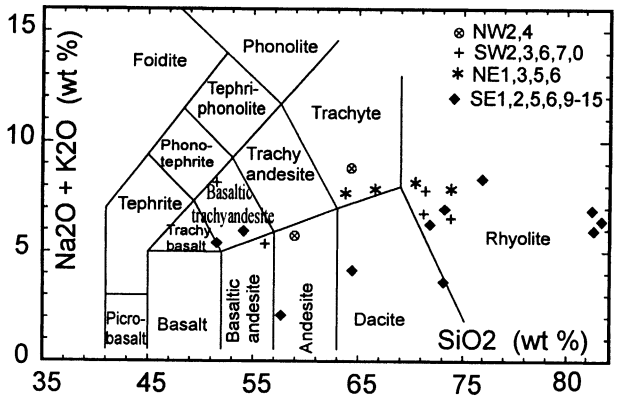

Figure 2. Chemical classification of the volcanic rocks around the Songliao Basin using total alkali versus silica (TAS). After Le Maitre *et al*. (1989, figure B13).

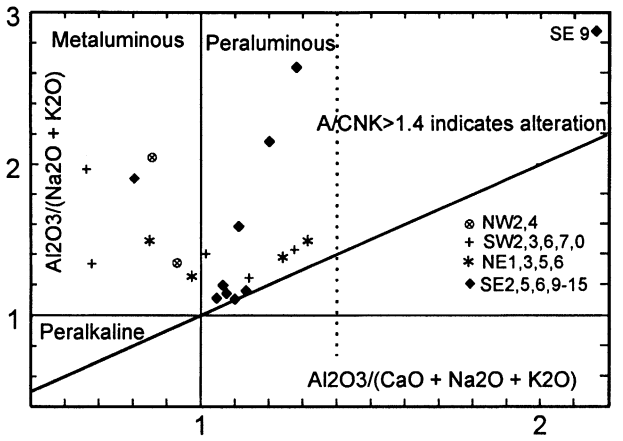

Figure 3. Shand's index of the volcanic rocks around the Songliao Basin. After Maniar and Piccoli (1989, figure 2).

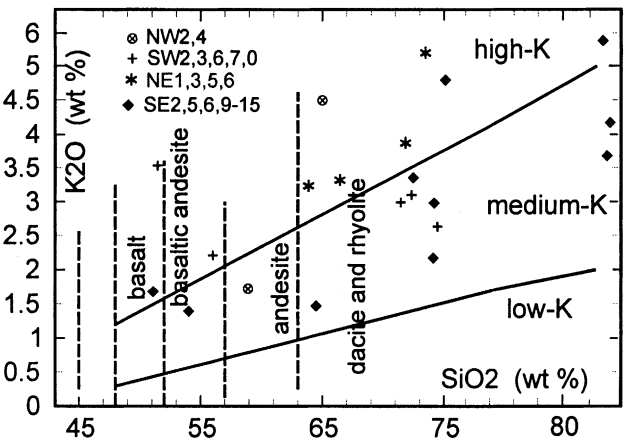

Figure 4. Series classification of the volcanic rocks around the Songliao Basin using sodium versus silica. After Le Maitre *et al*. (1989, figure B15).

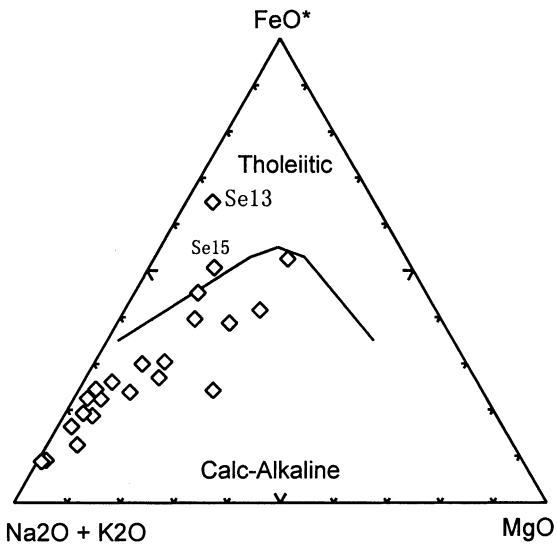

Figure 5. AFM plot of the volcanic rocks around the Songliao Basin. ($A = Na_2O + K_2O$; $F = FeO + 0.8998Fe_2O_3$; $M = MgO$). After Irvine and Baragar (1971, figure 2).

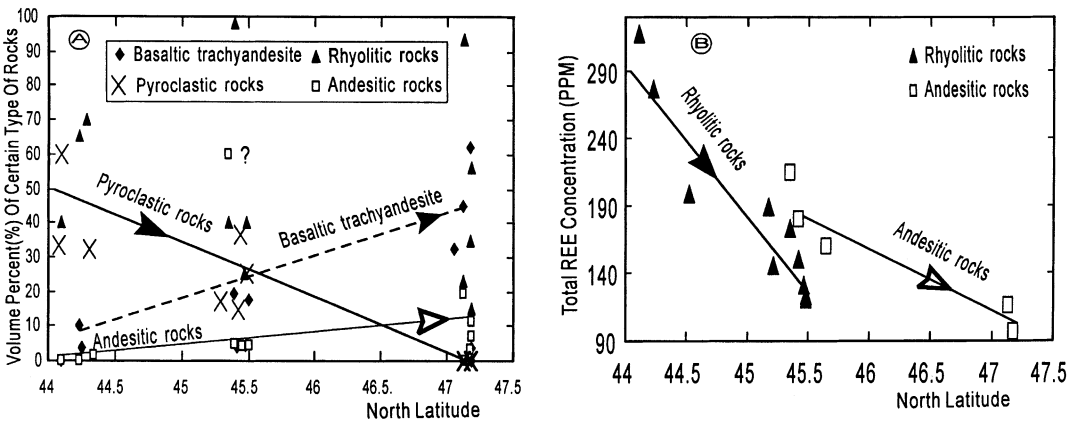

Figure 6. Lithologic associations (A) and total REE contents (B), showing change from south to north of the volcanic rocks around the Songliao Basin.

from south to north in the region. Rhyolitic rocks are in general abundant, but show irregular change in volume percentage latitudinally (Figure 6A).

The Early Cretaceous volcanogenic successions are lava flow facies and ignimbrites with interbeds of alluvial fan and fluvial deposits (Figure 1). Overlying the volcanics are sedimentary sequences of interbedded sandstone–siltstone–black shale with fluvial and lacustrine facies, which mainly developed within the SB.

5. GEOCHRONOLOGY OF THE VOLCANIC SUCCESSION AROUND THE SONGLIAO BASIN

5.1 K-Ar Isotopic dating and discussion on their reliability

K-Ar isotopic results are listed in Table 2 and the corresponding isochron ages are presented in Figure 7. The apparent K-Ar ages of the volcanics range from 139 to 113 Ma with analytical errors of 0.8–6.2 Ma. Isochron ages

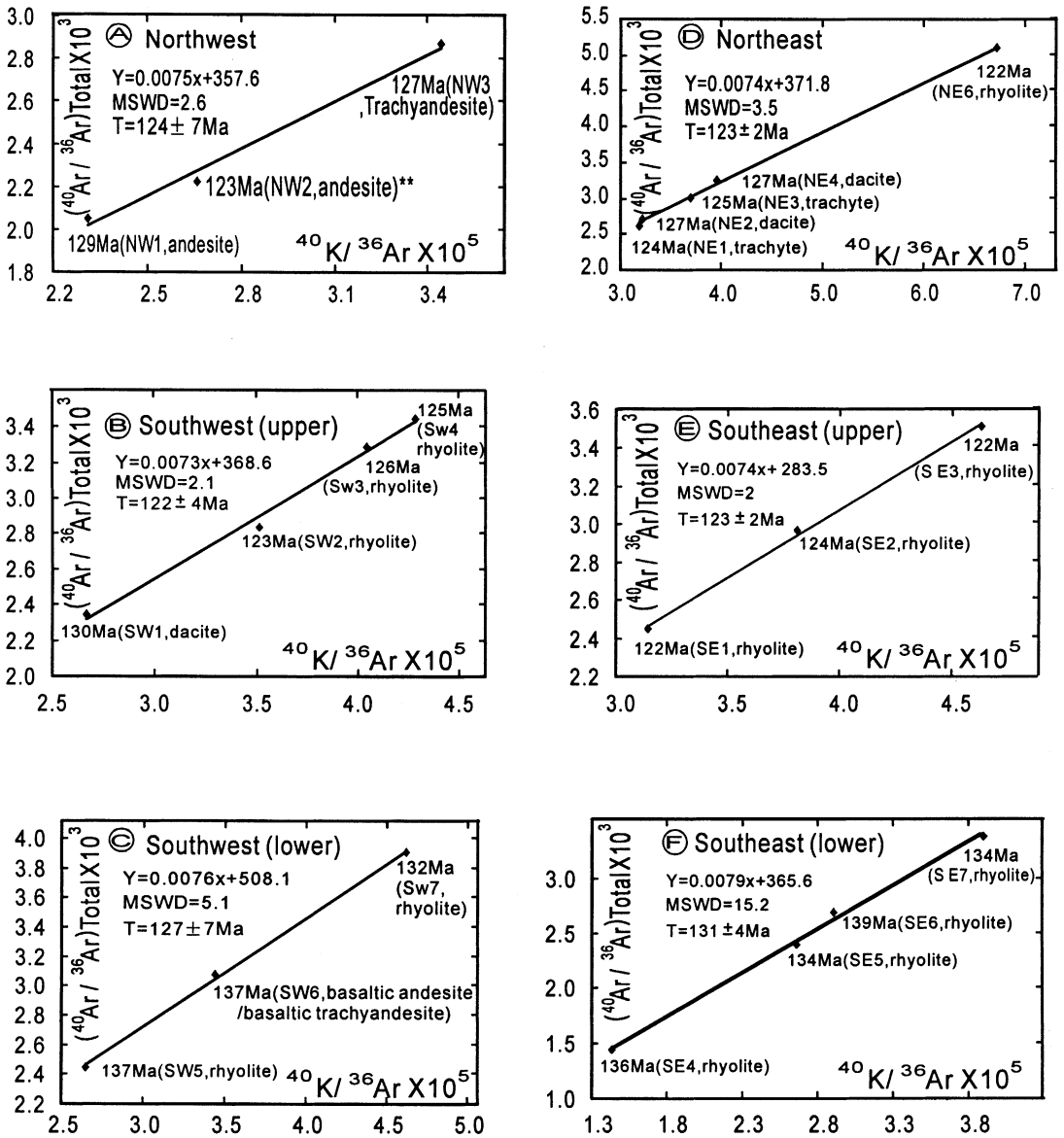

Figure 7. K-Ar isochron age plots for the volcanic rocks around the Songliao Basin. Isochron age (T) and mean standard weighted deviation (MSWD) were calculated with the program of Ludwig (1994). Sample number and rock type as in Table 2.

were processed with the group of samples collected from the same volcanic bodies that are from a single eruption cycle (recognizable on outcrops). Taking into account the analytical errors, the isochron ages are about in agreement with the single K-Ar data. However, three features should be noticed for the isochron ages in Figure 7, which are explained below. (1) Foremost, all the isochron ages are generally younger than those of the corresponding single K-Ar ages or nearly equal to the youngest ones. We would attribute this to extra argon incorporated into minerals or rocks at the time of crystallization, because the intercepts of those isochrons are greater than 295.5 (the initial $^{40}Ar/^{36}Ar$ in air). (2) For a certain isochron, samples with relatively younger ages have higher $^{40}K/^{36}Ar$ ratios and higher K contents (see Table 2) than their older counterparts do. (3) Samples with

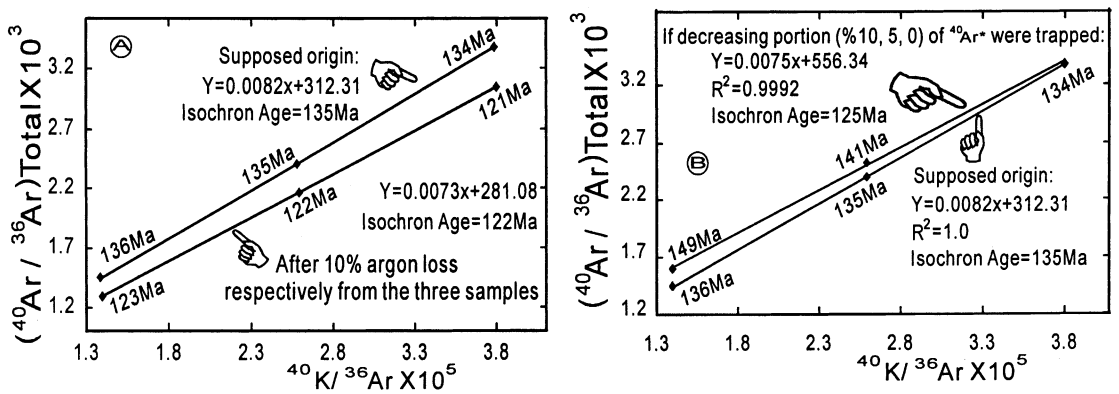

Figure 8. Models to explain why a K-Ar isochron age can be systematically younger than its 'true' age (135 Ma in the examples). (A) All kinds of argon are lost in equal proportion after cooling. (B) More inherited radiogenic argon is trapped at relatively early crystallization episodes.

abnormally high (or low) ages are above (or below) the mean isochron line (e.g. NW2, SW2 and SE6). Those anomalies may be caused by uneven argon entrapment as discussed below.

The K-Ar isochron diagram is theoretically effective in eliminating the effect of inherited argon (Dickin 1995, pp. 248–251) under the condition that the samples involved had the same initial $^{40}Ar/^{36}Ar$ and are closed systems with respect to K and Ar (Attendorn and Bowen 1997, pp. 199–201). However, several reasons can result in 'pseudochrons' such as (1) samples from different eruption cycle, (2) different initial $^{40}Ar/^{36}Ar$, and (3) alternation (i.e. compositional change after diagenesis consequent on weathering and/or reaction with subsurface fluids) of samples (A. Saunders, 2000, personal communication).

Samples used for the same isochron were collected from an equivalent layer of a single volcanic body in this case. It has been proved by field observations that they erupted synchronously. Special care was taken to exclude joint and cleavage surfaces, and veinlets from the analysed samples. Hand-picked samples of 20–40 mesh under the binocular microscope were used for age analysis. Samples with high A/CNK indexes over 1.4 (like SE9 in Figure 3) were excluded from age analysis since the A/CNK number of 1.4 is considered a critical value for recognizing chemical alterations (Siebel *et al.* 1997). We believe, therefore, that alterations, though commonly occurring, have been carefully excluded from the samples used for dating.

In order to determine the possible reasons for the systematically younger isochron ages in Figure 7, two illustrative models are shown in Figure 8. Figure 8A indicates that if argon loss happened after cooling, both single K-Ar ages (123–121 Ma) and the corresponding isochron age (122 Ma) will be apparently younger than its 'true age' (135 Ma). The intercept of its isochron decreased from 321.31 to 281.08. Figure 8B shows that if more radiogenic argon were trapped at earlier crystallization stages, which could reasonably happen because of less degassing at earlier episodes from the same batch of magma, the single K-Ar ages (e.g. 149 Ma and 141 Ma) will be older than its 'true age' (135 Ma); in contrast, the corresponding isochron age (125 Ma) will be much younger than either the mean single K-Ar age ($141.3 - 125 = 16.3$ Ma) or the 'real' cooling age ($135 - 125 = 10$ Ma).

Compared with the models of Figure 8, it seems that all the isochrons in Figure 7, except Figure 7E, show certain similarities with that of Figure 8B, suggesting a possible process of decreasing argon entrapment from early to late stages of crystallization. But their influence on the results is surely less than 10%, otherwise we would expect scattered ages more than 16 Ma between isochron age and mean K-Ar age as shown in Figure 8B. Considering the time difference (2–8 Ma) between isochron age and corresponding mean K-Ar age coupled with the extra argon revealed by the intercepts (508.1–357.6 Ma) of the isochrons in Figure 7, the uneven entrapment of initial argon should be within the level of *c*.5%. This is in the same level of analytical errors (*c*.4.5% on average; Table 2) which had to be considered in the isochron processing program (Ludwig 1994) used. We concluded, therefore, that differential entrapment of initial argon can be minimized to a level of *c*.5% if the samples are collected from an equivalent layer of a volcanic body and are lithologically similar (see the rock types in Figure 7). With the

discussions above and the comparisons with the ^{40}Ar-^{39}Ar incremental-heating and biostratigraphic data below, we can reasonably conclude that the K-Ar isochron results in Figure 7 are acceptable approaches to the cooling ages of the volcanics around the SB with cumulative errors estimated at no more than 10% (since the worst case is the sum of the two kinds of errors: analytical error of *c*.4.5 and error of *c*.5% from differential entrapment of initial argon).

5.2 Ar-Ar Radiometric dating and constraint on K-Ar results

For comparison with K-Ar results, three sets of samples collected from outcrops around the basin (marked on sections NE, SW and SE in Figure 1) were analysed for ^{40}Ar-^{39}Ar step-heating (Figure 9). Single crystals of sanidine, obtained by hand-picking under the binocular microscope, were used for the ^{40}Ar-^{39}Ar dating. The sample grains were selectively checked by electron microscope (JEM-2000FX, Japan) and the attached energy mass-spectrometer (TN-5500, USA). They proved to be fresh enough without recognizable alterations. Their plateau ages are 126 Ma, 133 Ma and 113 Ma with 93.7%, 92.5% and 93.6% of ^{39}Ar release respectively. These mean weighted ages can compare within errors of 2 Ma with the corresponding K-Ar isochron as well as K-Ar ages (127 Ma, 131 Ma and 115 Ma respectively; Figures 1 and 7).

The existence of extraneous argon of *c*.6–7% of ^{39}Ar release was revealed by the step-heating processes in that abnormally old ages were obtained at high temperatures as well as low temperatures (except for sample SWAr1126)

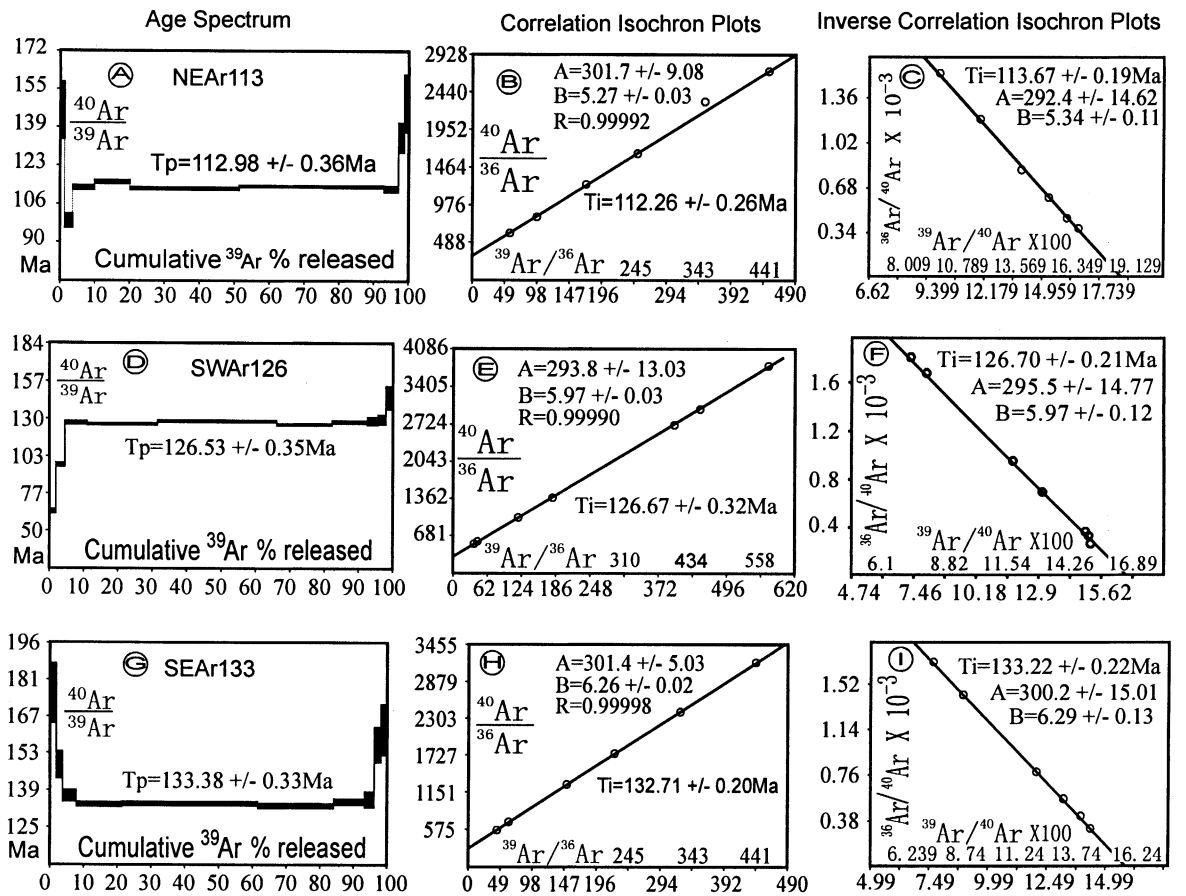

Figure 9. Flat release age spectrum (A, D, G) and corresponding correlation isochron plot (B, E, H) and inverse correlation isochron plot (C, F, I), for the volcanic rocks around the Songliao Basin. A = intercept; B = slope; R = distribution statistic number; J = constant obtained from standard; T (time) = 1.8041×10^9 Ln(J × B + 1).

in the ^{40}Ar-^{39}Ar age spectrum (Figure 9). Argon loss of 2.1–4.7% of ^{39}Ar release was also revealed by the ^{40}Ar-^{39}Ar age spectrum (NEAr113 and SWAr126). The total squares of extra argon (as well as argon loss) in the spectrum of Figure 9 occupy less than 10% of the whole spectrum square (Σ multiply ^{40}Ar-^{39}Ar age by ^{39}Ar release). So the single K-Ar ages in Table 2 can be expected to approach the volcanic cooling times with no more than 5% (7–2.1%) extra errors except analytical errors, although they are only the mixture ages after the argon trap and loss.

5.3 Constraints from fossil assemblages

Intercalated in the volcanogenic successions around the SB are some coal-bearing clastic deposits with alluvial/braided stream and fluvial facies. These interbeds occasionally contain fossils. For example, outcrop SE1p (Table 1) (cf. the middle unit of section SE in Figure 1), contained fossils in the coal-bearing tuffaceous/epiclastic rocks, including a pollen assemblage of *Piceites–Piceaepollenites;* megaspore species of *Maexisporites–Verrutriletes–Trileites*; late stage assemblage of flora *Ruffordia–Onychiopsis* including *Coniopteris onychioides, Cladophlebis* sp., *Elatocladus* sp., *Bralhyphyllum* sp., *Coniopteris* cf. *burrejensis*(Zal) *Seward*, *Palibiniopteris* sp., *Acanthopteis gothani vassil, Elatocladus manchurical*(Yok) Yabe, *Arctopteris rarineris samylina, Neozamites verchojianensis* Vach, *Taeniopteris* sp.; ostracoda assemblage of *Darwinula–Lycopterocypris*; bivalve assemblage of *Ferganoconcha–sibireconcha*; insecta assemblage of *Clypostemma* (Song *et al*. 1999). These fossil assemblages can be commonly found in other sections of the region and indicate a Cretaceous age according to regional stratigraphic correlation (Heilongjiang Geological Survey 1997; Jilin Geological Survey 1997).

6. GEOCHEMISTRY OF THE VOLCANICS AROUND THE SONGLIAO BASIN

6.1 Major elements

Correlation between major and some trace elements is shown in Harker diagrams (Figure 10). Amongst all the major elements, silica correlates positively only with potassium, and negatively with other elements (Figure 10). The points are generally more dispersed at lower SiO_2 content. There are no significant correlations amongst other elements in Table 3 except those shown in Figure 10. The Harker diagrams of Figure 10 consistently display the following features. (1) The volcanic suite defines a continuum of bulk compositions spanning the range from basaltic andesite to rhyolite. This indicates that the bulk compositions are primarily those of liquids, with accumulation of phenocrysts perturbing but not entirely swamping the important chemical trends (Hess 1989, p. 152). (2) Both Al_2O_3 and CaO concentrations as well as the ratios of CaO/Al_2O_3 decrease with SiO_2 contents, suggesting plagioclase appears early as a phenocryst phase. (3) Both TFeO and MgO decrease, and the TFeO/MgO ratio increases from basaltic andesite to rhyolite, being consistent with the fractionation of ferromagnesian minerals. (4) The TiO_2 and MnO contents decrease with SiO_2, suggesting a compatible behaviour of Ti and Mn probably because of the early crystallization of their oxides and/or clinopyroxene fractionation.

The positive correlation between Ca and Eu suggests the co-crystallization and substitution of the two elements. The transitional elements of Sc, V, Co and Ni decrease with SiO_2 content, suggesting compatible behaviour and affinity with Fe and Ti. The noteworthy trait of the positive correlation between Eu and MgO or TFeO (as well as TiO_2, MnO, Sc, V) may indicate that Eu became a compatible element and began its main episode of crystallization when such ferromagnesian silicates began to crystallize as diopside ($Ca(Mg, Fe)(SiO_2)_3$), hypersthene ($(Mg, Fe)SiO_3$), pyroxene ($(Ca, Na)(Mg, Fe)Si_2O_6$), hornblende ($NaCa_2(Mg, Fe)_4AlSi_6Al_2O_{22}(OH, F)_2$) and biotite ($K(Mg, Fe)_3AlSi_3O_{10}(OH, F)_2$). Some of these minerals exist as phenocrysts in the rocks (see Section 4). It can also be ascribed to plagioclase fractionation in a mixture of plagioclase and clinopyroxene crystallizing.

6.2 Trace elements

The incompatible-element data were plotted in order of decreasing incompatibility from left to right (Figure 11). The abundances were normalized to the average MORB values of Sun and McDonough (1989). The normalized

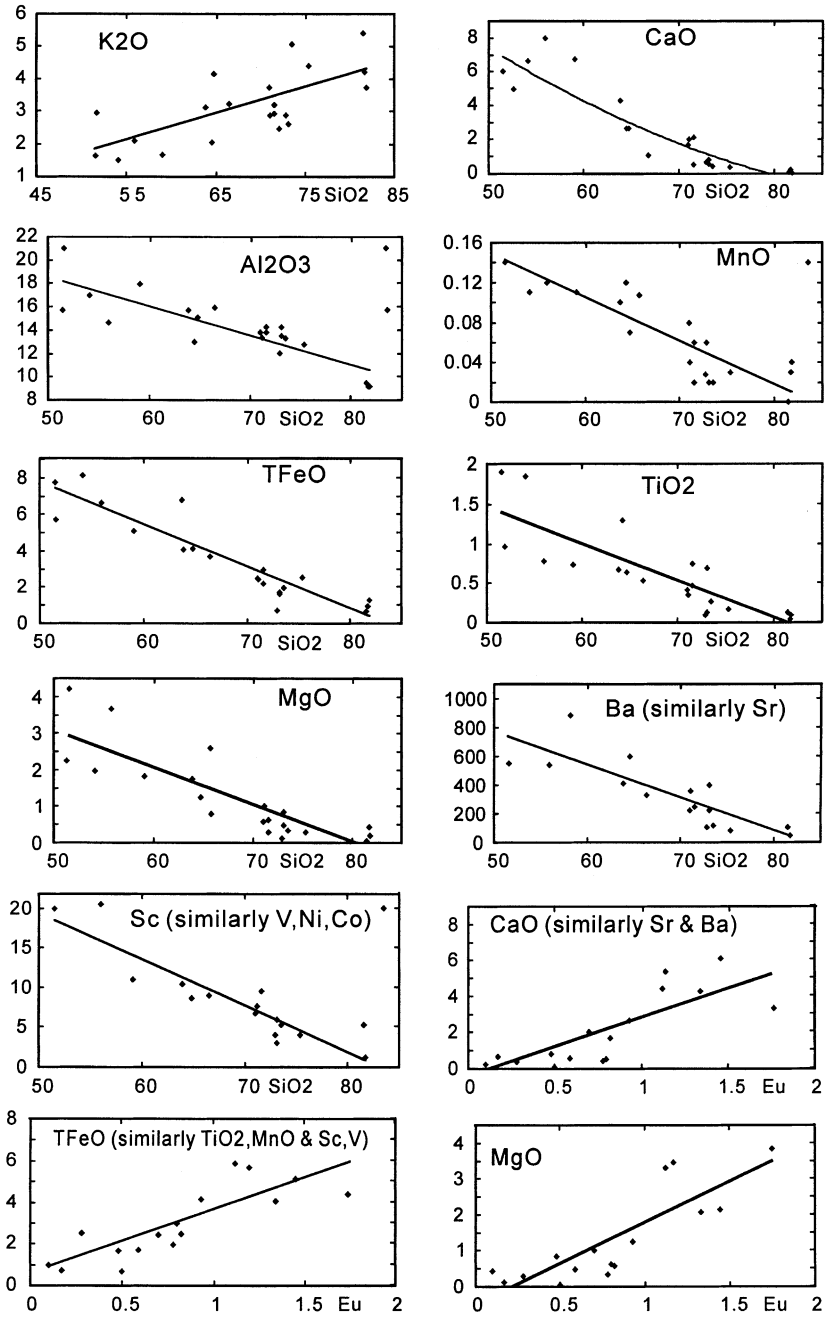

Figure 10. Harker diagrams for the volcanic rocks around the Songliao Basin. Major elements are in wt. % of their oxides, trace elements in parts per million.

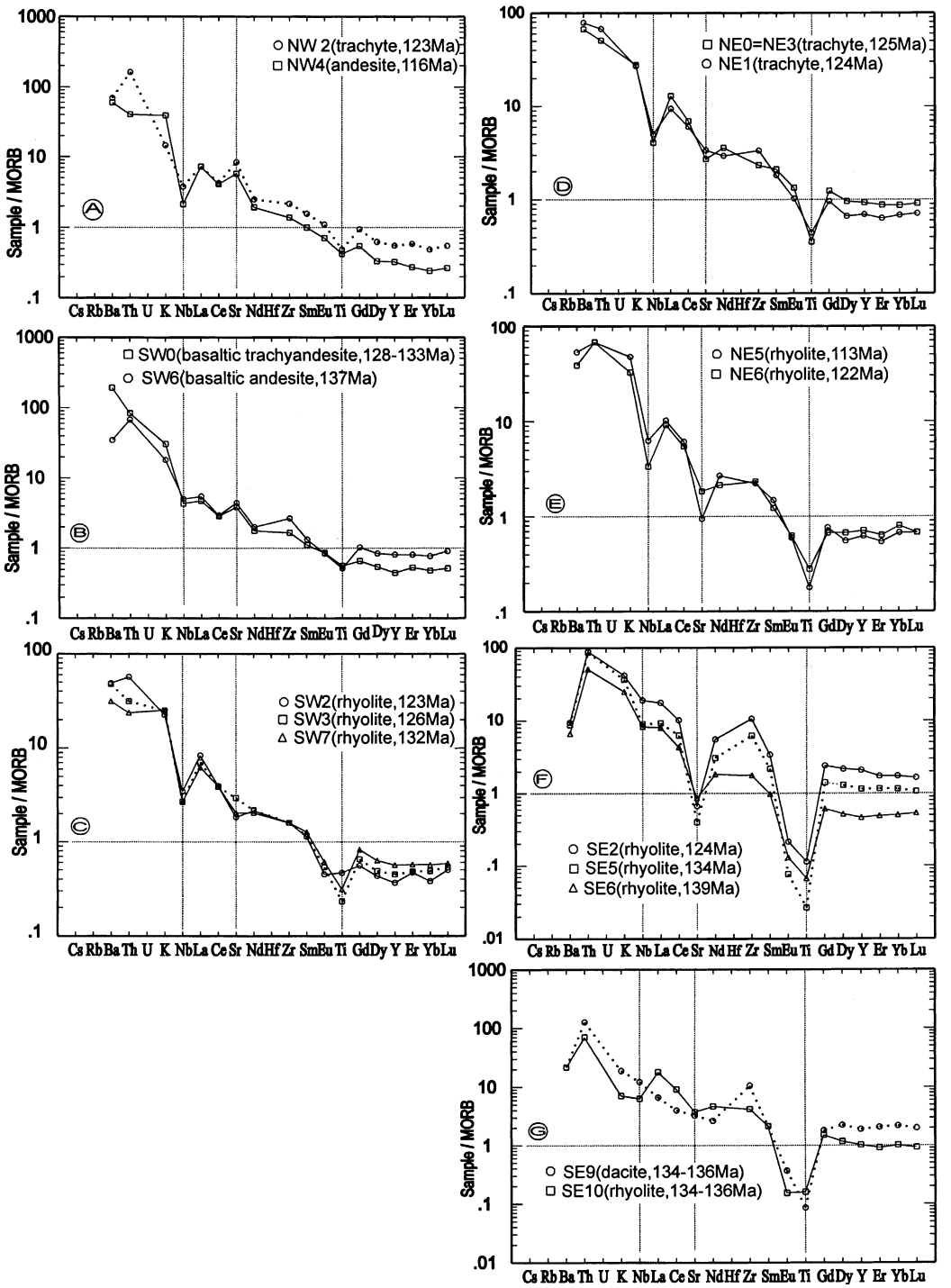

Figure 11. MORB-normalized multi-element plots for the volcanic rocks around the Songliao Basin. Normalization values after Sun and McDonough (1989).

curves slope down from left to right, indicating their enrichment in the more incompatible elements. They also show enriched large-ion lithophile elements (LILE; e.g. Ba, Th and K) and depleted high field strength elements (HFSE; e.g. Nb and Ti). Small positive Sr anomalies can be observed on the basic and intermediate volcanics from west of the SB (see Figure 11 A and B). However, most of the volcanic rocks show negative Sr anomalies especially for the rhyolites from east of the SB (see Figure 11 E and F).

The LREE are distinctly more enriched and fractionated than the HREE, being high in ΣLREE/ΣHREE (4.6–13.8, mean 8.8) and with chondrite-normalized ratios of La_{CN}/Sm_{CN} (2.9–4.6, mean 4.1) higher than those of Gd_{CN}/Yb_{CN} (0.9–2.3, mean 1.4) (Table 3). The HREE patterns are nearly flat slopes and depleted relative to MORB for most of the volcanics (see Figure 11). Negative Eu anomalies are in the range 0.04–0.88 of Eu/Eu* ratios. There are negative Ce anomalies (Ce/Ce* = 0.6–0.9, mean 0.82) for all the samples involved, suggesting highly oxidized environments of magmas which resulted in partially tetravalent and decreased ionic radius Ce (as described by Gill 1981, p. 132). Positive anomalies of Tb (Tb/Tb* = 0.7–2.6, mean 1.4) and Tm (Tm/Tm* = 0.7–2.2, mean 1.34) were commonly recognized. They may result from analytical error, but their concentrations are all significantly higher than the corresponding detection limits (Table 3), so that they possibly have geological significance.

It is noteworthy that REE contents in similar types of volcanics decrease from south to north in the region, showing a similar migrating trend to that of the lithologic associations (compare Figure 6A and B). For the same type of volcanics the ΣREE concentrations in the rocks decrease latitudinally. For different kinds of volcanic rocks, ΣREE in basaltic trachyandesite is the lowest (e.g. SW0, 96.1 ppm), while the youngest rhyolite from southeast of the SB has the highest REE content (e.g. SE2, 326.4 ppm).

7. THE RELATIONSHIP BETWEEN VOLCANISM AND BASIN EVOLUTION

7.1 Spatial and temporal affiliation of volcanic rocks with the Songliao Basin

The volume ratio is approximately 8:1:1.5 amongst acidic (rhyolite/perlite and dacite), intermediate (andesite, trachyte and trachyandesite) and basaltic volcanic rocks (basaltic andesite and basaltic trachyandesite) around the SB. Their exposed thickness ranges from 200 m to more than 2000 m and is about 730 m on average (see Table 1). On the other hand, the Cretaceous volcanic rocks recovered with drilling within the basin are rhyolite and dacite dominant (Gao and Xiao 1995) and have a revealed thickness of 100 m to 1200 m (mean *c*.550–680 m). The volcanics can be well correlated from the outcrops throughout the whole basin both geologically (petrography and texture) and geophysically (seismic reflection and well-logging) (Wang *et al*. 1992; Shao *et al.* 1999; Yang and Wang 1999).

Three episodes of volcanic activity around the basin were recognized according to the geochronologic results in this paper. They are dated 133–127 Ma, 124–122 Ma and 117–113 Ma, respectively (Figures 1, 7 and 9 and Table 2). Similarly, those in the basin are *c*.135 Ma, 126 Ma, and 113 Ma (Wang *et al*. 2002). Considering the analytical errors of 2–7 Ma, we can reasonably say that those volcanic activities occurred simultaneously both within and around the basin. The Cretaceous volcanogenic succession constituted the lower unit of basin filling, and proved to be one of the most important reservoir rocks for natural gas in the deeper part (3000 m below the surface) of the SB.

Distribution of the volcanic rocks both around and within the SB is different from that of their overlying sedimentary sequence striking NNE (represented as the present basin in Figure 1). For example, the maximum thickness of the volcanogenic succession was found on the southeast edge (over 2000 m thick, see SE1p in Table 1), instead of in the centre of the SB. Also, the first Cretaceous volcanic eruption (133 Ma) happened only in the southern part, while the last one (113 Ma) is found mainly in the north (see Sections SE and NW of Figure 1). This means that the volcanic activity migrated from south to north during the Cretaceous. In marked contrast, the overlying sedimentary sequence of Albian–Maastrichtian age is distributed in the northeast (cf. map of Figure 1) and the depositional centre migrated from east to west during sedimentation (Liu *et al*. 1993), which represents the typical tectonic regime of the circum-Pacific belt in this region. The south–north migrations of the lithologic associations and total REE contents of the volcanics in Figure 6 support the notion that a successively northward-stepping

volcanic series was formed in the Cretaceous in the area. Furthermore, on top of the Cretaceous volcanic succession was developed a regional angular unconformity, both around and within the basin (Figure 1; Wang *et al*. 1999). These facts indicate the existence of dynamic transformation in between the two super-sequences.

7.2 Volcanic petrogenesis and related tectonic setting

The bimodal-like successions of rhyolite–basaltic (trachy-) andesite (recognized on NW1p, NW2p and SE1p in Table 1) suggest the occurrence of fractional crystallization of basaltic magma and indicate the important role of magmatic differentiation in the petrogenesis. George Rowbotham (2001, personal communication) argued that bimodal succession can also be formed by crustal melting consequent on injection of basaltic magma. Initial isotope ratios of the Cretaceous volcanic rocks in the SB are in the range 0.70448–0.70660 ($^{87}Sr/^{86}Sr$) and 0.512300–0.512642 ($^{143}Nd/^{144}Nd$), indicating that only about 10% crustal components contributed to the magma source (Wang *et al*. 2002), so we can reasonably exclude the possibility of large-scale crustal melting in this case. The rhyolites with extremely large negative Eu anomalies (Figure 11) require that much feldspar is involved in the mineral/melt equilibria during melting or crystallization (Cullers and Graf 1984). To fit this, we should employ the two-stage models that include partial melting with much residual plagioclase in the magma source, and fractional crystallization of much plagioclase during magmatic differentiation (Condie 1978). Such great volumes of rhyolite of this kind are in general erupted along island arcs or continental margins (Hess 1989, p. 22). Although they could also result from melting of continental crust away from a continental margin (A. Saunders, 2000, personal communication), this does not fit our geological setting.

The major elements shown in Figure 10 possess the same features as those from island arc volcanic suites (Hess 1989, p. 153). The common occurrence of Ce anomalies ($Ce/Ce^* = 0.60–0.97$) may also compare with the volcanics of an island arc setting (Hawkesworth *et al*. 1994). On the other hand, the enrichment of highly incompatible elements such as K and Ba (Table 3 and Figure 11) are similar to those of continental margin volcanic series (Hess 1989, p. 168). The enrichment in LILE and LREE coupled with depletion in HFSE and HREE in the volcanics are indicative of subduction-related tectonic setting (e.g. Zanetti *et al.* 1999). The low contents of Ti and Ta and an enrichment in K and Rb in the relevant Mesozoic volcanics of northeast China also suggest a tectonic setting related to subduction (Zhao *et al*. 1998; Zhu *et al*. 1997).

7.3 Role of volcanism in basin evolution

The Cretaceous volcanogenic successions around and within the SB erupted during 133–113 Ma before the deposition of the overlying sedimentary sequence of Albian–Maastrichtian age (*c*.112–65 Ma). They were formed at the block-faulting stage and constituted the lower unit of basin filling of the SB. Basin opening accompanied the volcanic activities. It has been undoubtedly accepted that the overlying sedimentary sequence resting unconformably on the volcanics are tectonically controlled by the subduction of the Pacific Plate, because the model fits quite well with the main geological observations including its structural framework, the facies distribution and the vertical sequence (e.g. Wang *et al*. 1993; Liu *et al*. 1993; Gao and Xiao 1995). However, the genesis of the volcanic succession and its relation to the evolution of the SB is problematical.

Three representative ideas have been proposed for the role of volcanism in basin evolution of the region. (1) They are continental rift volcanics formed at the syn-rifting stage of the SB (e.g. Liu *et al.* 1993). (2) They are subduction-related arc volcanics and the formation of the SB resulted from the collapse of the orogenic belt (e.g. Zhao *et al*. 1998; Li *et al*. 1997). (3) They formed in an active belt of a spreading-type continental margin (Zhu *et al*. 1997). All three ideas attributed regional volcanism, directly or indirectly, to the subduction of the Pacific Plate under the Eurasian Plate with regard to their geodynamics.

Results shown in this paper, however, support an alternative explanation. Namely, they are subduction-related volcanic rocks and formed at an active continental margin that is related to subduction of the Mongolia–Okhotsk Plate under the North China Plate north of the SB during the Mesozoic, instead of subduction from the Pacific Plate east of the SB. Moreover, the overlying sedimentary sequence, by chance, was deposited unconformably upon the

volcanogenic succession, owing to the northwest oblique subduction of the Pacific Plate under the Eurasian Plate in the Albian–Maastrichtian (Zhang *et al*. 1999). There was a significant transformation of tectonic regime during 113–112 Ma in the region. That is to say, the Songliao Basin is just a kind of overlap basin with the two supersequences: the volcanogenic succession of up to 2000 m thick at its lower part and the overlying sedimentary sequence of up to 6000 m at its upper part. Both of them came together just because of the transformation of the tectonic regime in the region from the Mongolia–Okhotsk Ocean (in the north, before Albian) to the circum-Pacific (in the southeast, after Albian) in the Cretaceous.

Related evidence is summarized as follows. (1) The volcanics are predominantly calc-alkaline, metaluminous/peraluminous, intermediate-acidic suites (Figures 2–5), lacking basalts and peralkaline members that are typical of rift types (Hess 1989, pp. 263–275). (2) Initial isotope ratios of the volcanic rocks in the SB are in the ranges 0.70448–0.70660 ($^{87}Sr/^{86}Sr$), 0.512300–0.512642 ($^{143}Nd/^{144}Nd$), 17.758–18.223 ($^{206}Pb/^{204}Pb$) and 15.529–15.575 ($^{207}Pb/^{204}Pb$). In the plots of Sr-Nd isotope ratios and $^{206}Pb/^{204}Pb$ versus $^{207}Pb/^{204}Pb$, the samples plot between MORB and upper crust, fitting the hyperbolic mixing curve of two components with a K-value ($(Sr/Nd)_{Mantle}/(Sr/Nd)_{Crust}$) around 10 (Wang *et al*. 2000), which indicates an involvement of slab-derived components in their petrogenetic process. (3) The negative anomalies of Nb and Ti as well as Ta (cf. Zhu *et al*. 1997), coupled with the enriched LILE and LREE and depleted HFSE and HREE for most of the volcanics in Figure 11, are also indicative of a subduction-related setting (e.g. Zanetti *et al*. 1999).

The above characteristics of the volcanics can reasonably rule out the continental rift notion, but do not exclude a subduction from the Pacific Plate 1000–1500 km to the east of the SB.

Results in this paper and the regional geology and tectonics, however, show that the volcanism in the area migrated geochronologically and petrologically from south to north. The zonation is parallel to the Mongolia–Okhotsk collisional belt (200–600 km north of the SB). Thus, a successively northward-stepping Mesozoic volcanic series was obviously formed in the region. The palaeo-tectonic maps of the Yanshan area 100–300 km south of the SB show predominantly NEE and W-E structure lines for the Jurassic and Early Cretaceous and the main episode of magmatism is *c*.175 Ma (Zhao 1990, figures 1–4). The related fold axes and frontal faults trend roughly east to west, suggesting north–south shortening (Chen 1998). The studied volcanogenic successions regionally belong to Yanshanian volcanics (Cheng *et al*. 1990), but the main eruption time (131–113 Ma) is obviously later than those of the Yanshan Range, showing a northward-younging trend. Fisher and Schmincke (1984, pp. 384–385) believe that rock assemblages and their chemical composition can be broadly used as indicators of palaeotectonic environment. With distance from the subduction belt of oceanic crust, basaltic-andesitic rocks will decrease while rhyolitic-dacitic ignimbrites will increase because of the increasing involvement of continental lithosphere. For the same reason, we will expect an increasing trend of total REE content when it goes far from the subduction zone. From Figure 6 we can see that from south to north the percentage of pyroclastic rocks and total REE content in the same volcanic rocks decrease. This suggests that there is an increasing influence of oceanic crust and decreasing influence of continental lithosphere when going north; in other words it suggests subduction from the north. All these features as a whole support a dynamic motion more likely from the north, the Mongolia–Okhotsk collisional belt (Zorin 1999), than from the southeast, the Pacific Plate, during the eruption of the volcanics in the Mesozoic in the area.

8. CONCLUSIONS

The Cretaceous volcanics around the Songliao Basin are a series of high-K or medium-K, peraluminous or metaluminous, calc-alkaline rocks with eruption episodes of 133–127 Ma, 124–122 Ma and 117–113 Ma. They have high REE contents, are enriched in LILE and LREE and depleted in HFSE and HREE, with negative Nb, Ti, Eu and Ce as well as Ta anomalies and positive Tb and Tm anomalies. The Cretaceous volcanic rocks both around and within the Songliao Basin belong to the same suite in view of the petrography, geochronology, geochemistry and petrogenesis. Their geochemical signatures and the distribution patterns of the volcanics suggest that they formed at an active continental margin which is related to the closure of the Mongolia–Okhotsk Ocean to the north of the SB during the Mesozoic. The overlying sedimentary sequence, by chance, was deposited unconformably

upon the volcanogenic succession, owing to the northwest oblique subduction of the Pacific Plate under the Eurasian Plate during Albian–Maastrichtian time. The Songliao Basin is just a kind of overlap basin with the two super-sequences, the volcanogenic succession of up to 2 km thick at its lower part and the overlying sedimentary sequence up to 6 km thick at its upper part. The two units came together just because of the transformation of tectonic regime in the region from the Mongolia–Okhotsk Ocean (to the north of the SB, before Albian) to the circum-Pacific (to the southeast of the SB, after Albian) in the Cretaceous.

ACKNOWLEDGEMENTS

PuJun Wang is grateful to his German host professors, Professor Dr Gerhard Einsele and Professor Dr Muharrem Satir, for their kind help in the research. Special thanks to Professor Li You-Ming and Dr Liu Hong, directors of the project (NSFC49894190)–'Non-marine petroleum pool geophysics and 3D subsurface mapping', for their kind advice related to the research. PuJun Wang has benefited from discussions with Dr FuKun Chen. The authors thank Dr George Rowbotham and another referee for their constructive comments on the manuscript. The work was financially supported by the NSFC (Natural Science Foundation of China, project No. 49672124 and No. 49894190-13) and attained with the assistance of the AvH (Alexander von Humboldt Foundation, Germany).

REFERENCES

Attendorn H-G, Bowen RNC. 1997. *Radioactive and Stable Isotope Geology*. Chapman and Hall: London.

Chen A. 1998. Geometric and kinematic evolution of basement-cored structures: intraplate orogenesis within the Yanshan Orogen, north China. *Tectonophysics* **292**: 17–42.

Cheng YuQi, Shen YongHe, Ma QingYang (eds). 1990. *Geological Map of China (1:5000,000) and Guide Book*. Geology Press: Beijing (in Chinese).

Condie KC. 1978. Rare earth evidence for the origin of the Nuk gneisses Buksefjorden region, southern West Greenland. *Contributions to Mineralogy Petrology* **66**: 283–293.

Cullers RL, Graf JL. 1984. Rare earth element in igneous rocks of the continental crust: intermediate and silicic rocks-ore petrogenesis. In *Rare Element Geochemistry*, Henderson P (ed.). Elsevier: Amsterdam; 275–316.

Dickin AP. 1995. *Radiogenic Isotope Geology*. Cambridge University Press: London.

Fisher RV, Schmincke H-U. 1984. *Pyroclastic Rocks*. Springer-Verlag; Berlin.

Gao RiQi, Xiao DeMing. 1995. *Proceedings in Petroleum Exploration and Development of Daqing Oil Field*. Petroleum Industry Press: Beijing (in Chinese).

Gill JB. 1981. *Orogenic Andesites and Plate Tectonics*. Springer: Berlin.

Hawkesworth CJ, Gallagher K, Hergt JM, McDermott F. 1994. Destructive plate margin magmatism: geochemistry and melt generation. *Lithos* **33**: 169–188.

Heilongjiang Geological Survey. 1993. *Regional Geology of Heilongjiang Province of China*. Geology Press: Beijing (in Chinese).

Heilongjiang Geological Survey. 1997. *Lithostratigraphy of Heilongjiang Province of China*. Geosciences University Press: Wuhan (in Chinese).

Hess PC. 1989. *Origins of Igneous Rocks*. Harvard University Press: Massachusetts.

Irvine TN, Barager WRA. 1971. A guide to the chemical classification of the common volcanic rocks. *Canadian Journal of Earth Sciences* **8**: 523–548.

Jilin Geological Survey. 1988. *Regional Geology of Jilin Province of China*. Geology Press: Beijing (in Chinese).

Jilin Geological Survey. 1997. *Lithostratigraphy of Jilin Province of China*. Geosciences University Press: Wuhan (in Chinese).

Khudoley AK, Sokolov SD. 1998. Structural evolution of the northeast Asia continental margin: an example from the western Koryak fold and thrust belt (northeast Russia). *Geological Magazine* **135**: 311–330.

Le Maitre RW, with Bateman P, Dudek A, Keller J, Lameyre MJ, Lebas MJ, Sabine PA, Schmid R, Sorensen H, Streckeisen A, Wooley AR, Zanettin B. 1989. *A Classification of Igneous Rocks and Glossary of Terms*. Blackwell: London.

Li SiTian, Lu FengXiang, Lin ChangSong. 1997. *Ceno-Mesozoic Basin Evolution and Geodynamics of Northeast China and Adjacent Areas*. Dizhi Press: Beijing; 169–185 (in Chinese).

Liu ZhaoJun, Wang Dongpo, Liu Li, Liu WanZhu, Wang PuJun, Du XiaoDi, Yang Guang. 1993. Sedimentary characteristics of the Cretaceous Songliao Basin. *Acta Geologica Sinica* (English edition) **6**(2): 167–180.

Ludwig KR. 1994. *ISOPLOT-A Plotting and Regression Program for Radiogenic-Isotope Data (Version 2.75)*. Open-File Report 91–445, United States Geological Survey: Denver.

Mackenzie WS, Donaldson CH, Guilford C. 1982. *Atlas of Igneous Rocks and their Textures*. Longman: London.

Maniar PD, Piccoli PM. 1989. Tectonic discrimination of granitoids. *Geological Society of America Bulletin* **101**: 635–643.

Ross VR, Mercier J-CC, Xu YiGang. 1996. Diffusion creep in the upper mantle: an example from the Tanlu Fault, northeast China. *Tectonophysics* **261**: 315–329.

Sang HaiQing, Wang SongShan, Hu ShiLing, Qui Ji. 1997. 40Ar/39Ar dating method and Ar isotopic mass spectrometry analysis of quartz. *Journal of Chinese Mass Spectrometry Society* **15**(2): 17–27.

Scotese CR, Gahagan L, Larson RL. 1988. Plate tectonic reconstruction of the Cretaceous and Cenozoic ocean basins. *Tectonophysics* **155**: 27–48.

Shan XuanLong, Wang PuJun, Chen Shu-Mim, Ren YanGuang, Wan ChuanBiao. 1999. Stratigraphic correlation and tectonic significance on Upper Jurassic and Early Cretaceous in the Songliao Basin. *Journal of Changchun University Science and Technology* **29**(Special issue): 8–13 (in Chinese with English abstract).

Shao ZhengQui, Meng XiangLu, Wang HongYan, Wang PuJun. 1999. Seismic reflection and distribution of the Late Jurassic–Early Cretaceous volcanic rocks in the Songliao Basin. *Journal of Changchun University Science and Technology* **29**(1): 30–40 (in Chinese with English abstract).

Shelley D. 1995. *Igneous and Metamorphic Rocks under the Microscope: Classification, Textures, Microstructures, and Mineral Preferred Orientations*. Chapman & Hall: London.

Siebel W, Raschka H, Irber W, Kreuzer H, Lenz K-L, Hoehndorf A, Wendt I. 1997. Early Palaeozoic acid magmatism in the Saxothuringian belt: new insights from a geochemical and isotopic study of orthogneisses and metavolcanic rocks from the Fichtelgebirge, SE Germany. *Journal of Petrology* **38**: 203–230.

Song TingGuang. 1997. Inversion styles in the Songliao Basin (northeast China) and estimation of the degree of inversion. *Tectonophysics* **283**: 173–188.

Song WeiHai, Wan ChuanBiao, Bian, WeiHua, Shan XuanLong, Wang PuJun. 1999. Biostratigraphy and stratigraphic correlation of the Jurassic & Early Cretaceous in the Songliao Basin and adjacent areas. *Journal of Changchun University Science and Technology* **29**(Special issue): 62–69 (in Chinese with English abstract).

Sun SS, McDonough WF. 1989. Chemical and isotopic systemics of oceanic basalts: implications for mantle composition and processes. In *Magmatism in Ocean Basins*, Saunders AD, Norry MJ (eds). Geological Society, Special Publication **42**: 313–345.

Wang PuJun, Du XiaoDi, Wang DongPo. 1992. Categories and characteristics of Songliao Basin Cretaceous logging-sedimentary facies. *Journal of Changchun University Science* **22**(2): 169–179 (in Chinese with English abstract).

Wang PuJun, Wang HongBin, Song WeiHai. 1997a. Volcano related sedimentary basins and oil and gas reservoirs, NE China. In *Proceedings for the 4th Korea–China Joint Geology Symposium on Crustal Evolution on Northeast Asia*, Jang BA, Cheong DK (eds). Kongwan University Press: Chunchen; 109–115.

Wang PuJun, Chang Ping, Li Hong, Wang DongPo. 1997b. Sequential analysis of oil shales and its application to biomineralization research. *Experimental Petroleum Geology* **19**(4): 382–387 (in Chinese with English abstract).

Wang PuJun, Wang ShuXue, Qu YongBao, Ren YanGuang. 1999. Volcanic events of the Cretaceous Songliao Basin—a case study of Yingcheng Formation. *Journal of Changchun University Science and Technology* **29**(Special issue): 50–55 (in Chinese with English abstract).

Wang PuJun, Satir M, Mattern F. 2000. Sr, Nd, Pb and O isotopes of volcanic rocks in the Songliao Basin (SB), NE China: constraint on tectonic setting. *European Journal of Mineralogy* **12**: 228.

Wang PuJun, Liu WanZhu, Wang ShuXue, Song WeiHai. 2002. 40Ar/39Ar and K/Ar dating on the volcanic rocks in the Songliao Basin, NE China: constraints on stratigraphy and basin dynamics. *International Journal of Earth Sciences* **91**(2): 1–12.

Wang SongShan, Liu JiaQi, Zhu Ming, Zhao DongZhi. 1983. K/Ar and $^{40}Ar/^{39}Ar$ isotopic dating on the Cenozoic volcanic rocks from Changbaishan mountain. *Scientia Geologica Sinica* **3**: 205–215 (in Chinese with English abstract).

Wang YuJing, Fan ZhiYong. 1997. Discovery of Permian radiolarians in ophiolite belt on northern side of Xilamulun river, Nei Monggu, and its geological significance. *Acta Palaeontologica Sinica* **36**(1): 58–69.

Wang ZhiWu, Yang JiLiang, Gao RiQi (eds). 1993. *Petroleum Geology of Daqing Oil Field*. Petroleum Industry Press: Beijing (in Chinese).

Xu JiaWei, Ma GuoFeng. 1990. Review of ten years (1981–1991) of research on the Tancheng-Lujiang fault zone. *Geological Review* **38**(4): 316–322 (in Chinese with English abstract).

Yang BaoJun, Wang PuJun. 1999. Study on T_3, T_4 and T_5 seismic reflection and their geological significance in the Songliao Basin. *Journal of Changchun University Science and Technology* **29**(Special issue): 13–20 (in Chinese with English abstract).

Zanetti A, Mazzucchelli M, Rivalenti G, Vannucci R. 1999. The Finero phlogopite-peridotite massif: an example of subduction-related metasomatism. *Contributions to Mineralogy and Petrology* **134**: 107–122.

Zhang MeiSheng, Sun XiaoMeng, Peng XiangDong, Zhang SongMei. 1999. Mesozoic tectonic stages of the Songliao Basin and adjacent regions. *Journal of Changchun University Science and Technology* **29**(Special issue): 20–24 (in Chinese with English abstract).

Zhao HaiLin, Deng JinFu, Chen FaJing, Hu Quan, Zhao ShiKe. 1998. Petrology of the Mesozoic volcanic rocks and the basin formation in northeast China. *Geoscience* **12**(1): 56–62 (in Chinese with English abstract).

Zhao XiXi, Coe RS, Zhou YaoXiu, Wu HaoRuo, Wang Jie. 1990. New paleomagnetic results from northern China: collision and suturing with Siberia and Kazakhstan. *Tectonophysics* **181**: 43–81.

Zhao Yue. 1990. The Mesozoic orogenies and tectonic evolution of the Yanshan area. *Geological Review* **36**(1): 1–13 (in Chinese with English abstract).

Zhu QinWen, Lu FengXiang, Xie YiHong, Zheng JianPing. 1997. Volcanic rock assemblages in active belts of spreading type in continental margins; study on Mesozoic volcanic rocks around Songliao Basin. *Acta Petrologica Sinica* **13**(4): 551–562 (in Chinese with English abstract).

Zorin YA. 1999. Geodynamics of the western part of the Mongolia–Okhotsk collisional belt, Trans-Baikal region (Russia) and Mongolia. *Tectonophysics* **306**: 33–56.

Scientific editing by Ian Somerville.

